analytical chemistry

ARTICLE

pubs.acs.org/ac

Frequency Dependence of Alternating Current Electrospray Ionization Mass Spectrometry

Nishant Chetwani,[†] Catherine A. Cassou,[‡] David B. Go,[*,§] and Hsueh-Chia Chang[*,†]

[†]Chemical and Biomolecular Engineering, University of Notre Dame, Notre Dame, Indiana 46556, United States

[‡]Department of Chemistry, University of California, Berkeley, California 94720, United States

[§]Aerospace and Mechanical Engineering, University of Notre Dame, Notre Dame, Indiana 46556, United States

Supporting Information

ABSTRACT: The novel effects resulting from the entrainment of low mobility ions during alternating current (ac) electrospray ionization are examined through mass spectrometry and voltage/current measurements. Curious phenomena such as pH modulation at high frequencies (>150 kHz) of an applied ac electric field are revealed and explained using simple mechanistic arguments. Current measurements are utilized to supplement these observations, and a simplified one-dimensional transient diffusion model for charge transport is used to arrive at a scaling law that provides better insight into the ac electrospray ionization process. Moreover, because of the different pathway for ion formation in comparison to direct current (dc) electrospray, ac electrospray (at frequencies >250 kHz) is shown to reduce the effects of ionization suppression in a mixture of two molecules with different surface activities.

Over the past few decades, significant attention been directed toward experimental and theoretical studies on direct current (dc) electrosprays,[1−4] in large part due to their production of charged liquid aerosols and their application as a soft ionization technique for large biomolecules in mass spectrometry.[5,6] These efforts have resulted in the development of a multitude of theories on the mechanism of dc electrosprays, especially on the most predominantly used "cone-jet" mode.[7,8] Apart from the development of electro-hydrodynamic models to explain the static Taylor's cone, scaling laws that estimate the droplet size distribution and parametric dependence of current have been important in optimization for mass spectrometry applications.[9,10] In contrast to the dc electrospray that is formed on an application of a dc electric field, a fundamentally different ac electrospray is formed by applying a high-frequency alternating current (ac) electric field,[11−13] and it has been recently demonstrated as an ionization source for mass spectrometry.[14] Thus far, there has been no analysis on ac electrospray that comprehensively aims at understanding the ionization mechanism and correlating it with effects important for applications in mass spectrometry.

dc electrosprays are formed as a consequence of the electrophoretic force due to the application of a high external dc electric field, which separates positive and negative charges in an electrolyte solution. This electrophoretic force leads to the deformation of the liquid meniscus into a sharp, conical tip known as a Taylor cone, and all of the charges within the liquid cone are rapidly ejected in the form of charged droplets. As such, there is no net charge build-up in the cone itself, and the electrostatic stress (often called Maxwell pressure) generated due to the interfacial polarization balances the surface tension to further sustain the cone.[1,7] Analyte ionization, such as deprotonation/protonation, ion-pair association/condensation, and adduct formation, then predominantly occurs in the gas-phase via desorption of molecules from the charged droplets (ion evaporation model) or Rayleigh fission of the droplets. In contrast to this mechanism, an ac electrospray is formed when a high-frequency ac electric field is applied to the liquid, and the cone formation is dependent on both the ionization and separation of analyte molecules in the cone itself,[11−14] a fundamentally different phenomenon than dc electrospray ionization (ESI).

The mechanism that leads to the formation of ac electrosprays, which we refer to as preferential entrainment, can be well understood by examining the two ac half cycles, the anodic and cathodic half cycle, separately (see Figure 1). We consider an example of an acidified protein solution to analyze the ionization process and the motion of ions under the action of two half cycles of an ac electric field. During the anodic half cycle, the protons migrate electrophoretically toward the meniscus while the protein molecules are driven hydrodynamically toward the meniscus and associate with the protons to form a protonated protein ion in the liquid phase, a phenomena which we refer to as "cone ionization" that is distinct from the gas-phase dc ionization pathway. During the cathodic half cycle, the free protons are driven back away from the meniscus toward the counter electrode. The low mobility protein ions, whose Maxwell relaxation time scale (given by λ^2/D, where λ is the double layer thickness and D is the diffusion coefficient[15]) is much higher than the time scale corresponding to the frequency of the ac electric field (given by $1/f$, where f is the frequency of the applied ac electric field) do not relax toward the counter electrode. A detailed description on the relative value of these time scales and its effect is provided in

Received: December 5, 2010
Accepted: February 21, 2011
Published: March 21, 2011

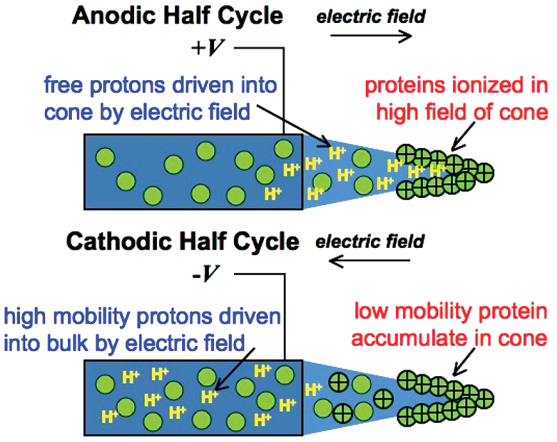

Figure 1. Schematic of the ionization and entrainment phenomenon in ac electrospray ionization.

detail in the ensuing sections of this work. Therefore, because of this phenomenon of "preferential entrainment", the low mobility protein ions remain confined in the vicinity of the meniscus , as shown in Figure 1. Hence, during the complete ac cycle, there is ionization and accumulation of large protein molecules in the meniscus. After many such cycles, the electrostatic repulsion between the net space charge (due to protein ions) balances the capillary forces and results in an ac cone that not only has a more slender half angle of ~12° than its dc Taylor counterpart (~49°) but that also continuously grows in time.[12,13]

In the authors' prior work,[14] ac ESI was shown to be a soft ionization technique for biomolecules in both positive and negative mode mass spectrometry that generally produced higher signal intensity than dc ESI. It was postulated that the increased signal intensity in ac electrospray ionization (ac ESI) was due in large part to the cone ionization and preferential entrainment phenomena that increased the concentration of the target analyte in the cone. A secondary effect the authors' identified was the more efficient transport of ions into the mass spectrometer because ac ESI emits a more confined plume of droplets. However, both of these potential effects need to be explored in more depth. The present manuscript aims to provide greater insight into the preferential entrainment and cone ionization processes by exploring the frequency-dependent characteristics of ac ESI. Features including pH modulation, voltage−current relationships, and ionization suppression are all presented.

EXPERIMENTAL METHODS

The representative proteins cytochrome c (molecular mass $M \sim 12\,400$ Da) and myoglobin (molecular mass $M \sim 17\,000$ Da) were obtained from Sigma Aldrich (St. Louis, MO). Tetrabutyl ammonium iodide (molecular weight 369.4) and tetrapentyl ammonium iodide (molecular weight 425.5) were purchased from MP Biomedicals (Solon, OH). Stock solutions of myoglobin and cytochrome c at a concentration 1 mM were prepared in deionized (DI) water and further diluted in different mixtures of acetonitrile (ACN) (Sigma Aldrich) and DI water in ratio 1:1 (v/v). The pH ranged from 2.75 to 4.5 (monitored using pH meter) through the addition of varied quantities of formic acid (HCOOH) to yield a 10 μM sample for mass spectrometric analysis. Similarly, stock solutions of 1 mM tetrabutyl ammonium iodide and tetrapentyl ammonium iodide were prepared in ACN and diluted in 1:1 ACN/DI water solution to yield a sample solution with a concentration of 20 μM, which was used for experiments.

Mass spectra were collected on an Esquire 3000+ spectrometer (Bruker Daltonics Inc.) equipped with a quadrupole ion trap (QiT) mass analyzer. A customized ionization chamber door was developed so that the ESI emitter was oriented axially to the mass spectrometer inlet, and this was used for back-to-back comparison between ac and dc ESI experiments. Nitrogen gas (N_2) was used as a nebulizing gas at a pressure of 10 psi to aid droplet formation and stabilize both the ac and dc electrosprays. Counter-flow drying gas (N_2) was used at a flow rate of 3 L/min to enhance desolvation, and a sample flow rate of 0.3 mL/h was used for all experiments. For dc ESI experiments, protein samples with different pH were injected into the mass spectrometer by directly applying a dc potential ~2 kV onto the emitter using an external power supply (Matsusada Precision ES-5R1.2), keeping the end plate at ground (0 V) and capillary inlet to the mass spectrometer at an offset of −500 V. Mass spectra were acquired for 10 min. For ac ESI experiments, the protein sample at a single pH of ~2.95 was used at frequencies and root-mean-square (rms) voltages ranging from 50 to 400 kHz and 0.6 to 1.4 kV_{rms}. The ac potential was applied using a function generator (Agilent 33220A) connected to a radio frequency (rf) amplifier (Industrial Test Equipment 500A) and a custom-made transformer (Industrial Test Equipment Co.). The same procedure was employed for the analysis of quaternary ammonium salts. It should be noted that for accurate measurements of intensity, ion current gain was switched from an automatic acquisition time of 200 ms/spectrum (and ion current target of 20 000) to 10 ms/spectrum.

Current/voltage measurements were also conducted independently of the mass spectrometry measurements using the same electrospray emitter (at the same flow rate and nebulizer gas pressure) and a copper plate counter electrode spaced ~1 cm apart. The copper plate was maintained at ground (0 V), and ac potential was applied directly to the electrospray emitter. The circuit was grounded to a hard-wired earth ground in the laboratory that led outside of the building. The current was recorded using a picoammeter (Keithley 6485), and the emitter voltage was measured with an oscilloscope (Tectronix TDS2014) coupled with a high voltage probe. Protein samples at pH 2.75 were studied at frequencies ranging from 50 to 170 kHz, and the current was recorded at an interval of 0.2 s for ~5 min. After this time period, the current magnitude started to reduce gradually due to the deposition of unevaporated liquid on the counter electrode and no further measurements were made.

RESULTS AND DISCUSSION

Frequency Dependence and pH Modulation. Figure 2a shows a characteristic ac rms voltage−frequency phase space for the mass spectrometry (MS) experiments. Three distinct regimes can be identified in Figure 2a: (i) below onset regime, the regime below the onset rms voltage in which no signals were observed and only noise was recorded. (ii) Operating regime, the stable operation regime, with voltage greater than the onset voltage, in which MS signals corresponding to the analyte ions, distinct from noise, were observed as shown in Figure 2b. (iii) Discharge regime, the regime beyond the threshold rms voltage in which the peaks corresponding to the apo myoglobin ions disappeared

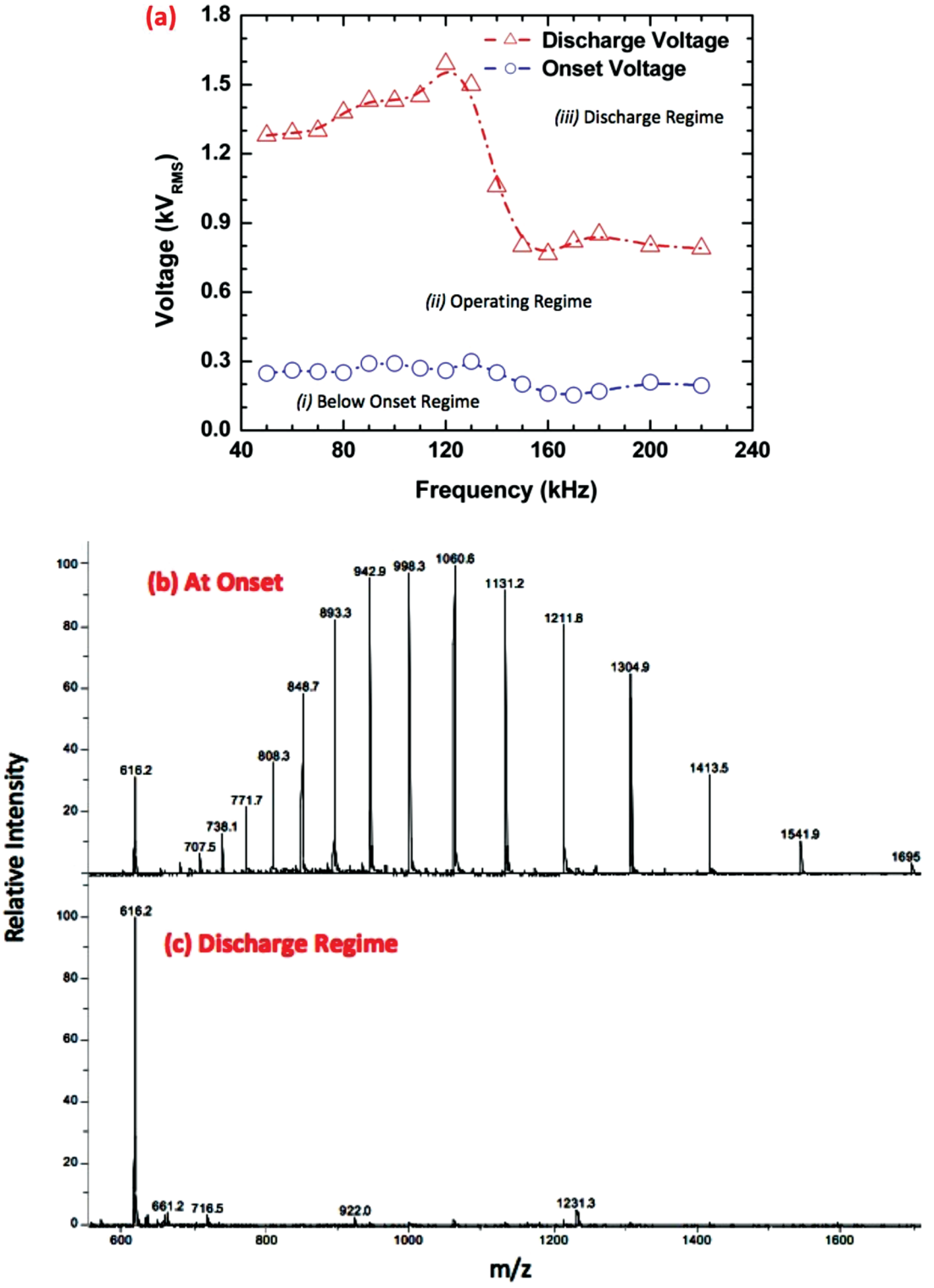

Figure 2. (a) Frequency−voltage phase space for myoglobin (10 μM) indicating the operating regime bounded by onset voltage and discharge voltage. (b) Mass spectrum showing the multiple peaks of apo-myoglobin (10 μM) at 80 kHz and 0.35 kV_{rms}. (c) Mass spectrum showing the intense peak of the heme group ($m/z \sim 616$) at 80 kHz and 1.38 kV_{rms}.

and only the heme group was observed, as evident in Figure 2c. Thus two critical voltages, onset and discharge, bound the operating regime for ac ESI mass spectrometry. The discharge regime in ac ESI is characterized by a corona discharge with a strong confined glow at the tip of the emitter, which can be directly visualized in the dark. The disappearance of apo-myoglobin peaks during MS in the discharge regime can be compared with corona discharge-driven atmospheric pressure chemical ionization (APCI) MS, where only low molecular weight proteins (~600 Da) are observed while higher molecular weight

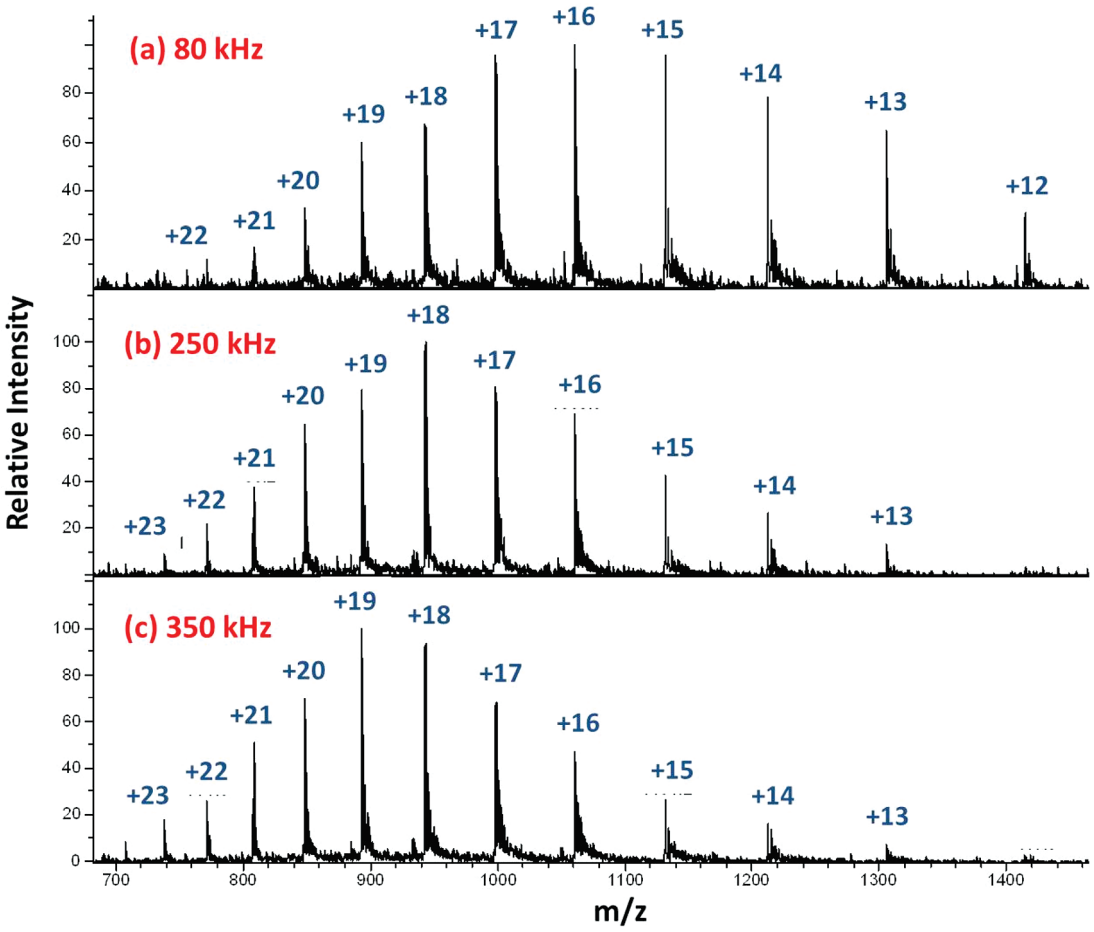

Figure 3. Mass spectra indicating the shift in charge states of apo-myoglobin (10 μM) at pH 3 and (a) 80 kHz and 0.95 kV_{rms}, (b) 250 kHz and 0.7 kV_{rms}, and (c) 350 kHz and 0. 55 kV_{rms}.

proteins do not appear at all.[16] This is possibly the case observed here with ac ESI MS in the discharge regime where only the low molecular weight species, heme group ($m/z \sim 616$) was observed, while the peaks corresponding to the large apo-myoglobin disappear completely. The alternate plausible mechanism for the disappearance of apo-myoglobin peaks in the discharge regime is due to the creation of bigger charged droplets when the corona discharge is formed.[11] Given that the heme group is highly hydrophobic and that the remaining apo-myoglobin is hydrophilic in nature, it is hence more favored for the formation of the ion during the flight of the charged droplet and hence is recorded in the mass spectrum. On the other hand, the apo-myoglobin molecule occupies the liquid bulk of a charged droplet and therefore cannot form a gas phase molecular ion, potentially leading to its disappearance in the discharge regime.

Apart from the strange disappearance of the apo-myoglobin peak from the mass spectra in the discharge regime, there was also anomalous behavior of the mass spectra by varying the frequency in the stable operating regime. For apo-myoglobin, a near symmetric Gaussian distribution of the multiply charged peaks, centered at a charge state value of +13, is typically observed for dc ESI at pH of 4.1. As the pH is reduced, the symmetric Gaussian distribution becomes skewed; with the mode moving toward higher charge states and the peak of the charge state distribution shifting to a value of +16 at a pH of 2.75.[17] This occurs because at lower pH the protein molecule unfolds, which allows for a larger degree of protonation and consequently leads to higher charged states in the mass spectrum.[18,19] When using ac ESI for myoglobin at a pH of 2.95, a behavior similar to dc ESI is observed at low frequencies (~50 kHz), with the peak of the distribution centered at +16. However, as the frequency is increased, the distribution continues to skew and the peak shifts toward higher charge state values as shown in Figures 3 and 4. For example, at frequencies ~350 kHz or higher, the peak of the charge state distribution is +19 (Figure 3c). This curious frequency-dependent behavior may again be attributed to the entrainment characteristic of ac ESI. As the frequency increases, a greater number of half cycles occur over a given time window, and more protons are periodically driven into and out of the cone, while the low mobility charged protein molecules accumulate near the meniscus after every cathodic half cycle. As such, this to and fro motion of protons enhances their chance to attach to an already protonated protein molecule, thereby increasing its charge state. Effectively, as the frequency increases, the local pH at the tip of the cone is reduced because of a greater influx of protons into the cone, thus resulting in the significant shift of analyte peaks in the mass spectra. Similar effects for cytochrome-c (not shown) were also observed to confirm this charge state effect.

Current Measurements and Scaling Analysis. To further clarify how the entrainment effect may modulate pH, current measurements were carried out at different frequencies but

dx.doi.org/10.1021/ac103189p |*Anal. Chem.* 2011, 83, 3017–3023

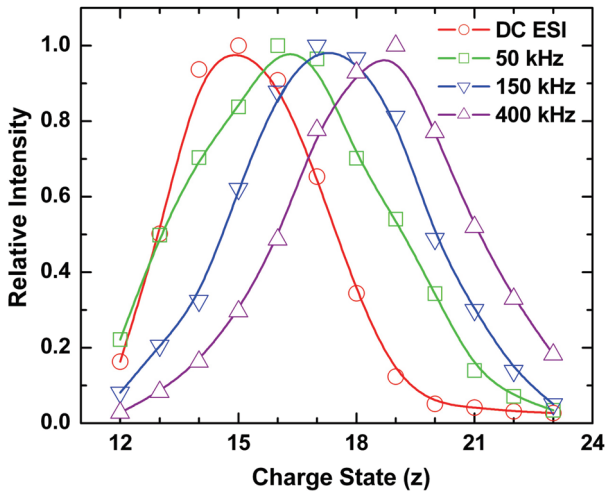

Figure 4. Charge state distributions of apo-myoglobin (10 μM) for different frequencies using the same nominal pH.

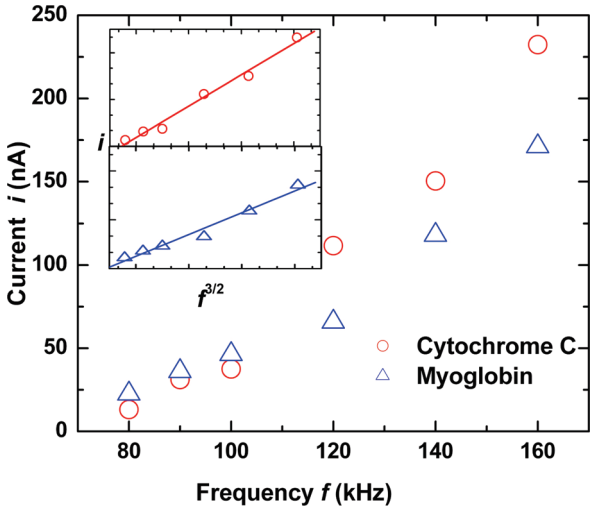

Figure 5. Current-frequency (i–f) characteristic for myoglobin and cytochrome c. The inset shows the linear fit of i with respect to $f^{3/2}$, each with regression coefficients of determination $R^2 > 0.98$.

constant rms voltage. These measurements showed a monotonically increasing trend of current with frequency (Figure 5). In order to investigate this trend, we carry out a simplified scaling analysis of ion transport in the ac cone. To arrive at the governing equations, we return to the mechanism of formation of ac electrosprays described earlier in the present report. While the ionization of apo-myoglobin molecules primarily occurs during the anodic half cycle, diffusion can be assumed to be the primary means of transport of charged apo-myoglobin molecules during the cathodic half cycle owing to their low mobility, while the high mobility free protons are electrophoretically driven toward the counter electrode. Therefore, the distribution of protein ions in the cone during the cathodic half cycle can be described by the classical diffusion equation,

$$\frac{\partial \rho}{\partial t} = D\frac{\partial^2 \rho}{\partial x^2} \tag{1}$$

where ρ is the charge density corresponding to that of protonated protein ions, t is the time, D is the diffusion coefficient of the proteins, and x is the coordinate direction along the axis of the cone. Additionally, it is assumed that the protonation occurs at the tip of cone so that the resulting charge q that is generated by ionization after each anodic half cycle can be considered to be a point charge. This serves as the initial condition when the cathodic half cycle begins and can be mathematically represented by a Dirac delta function of value q. Additionally, since the dimension of the fluid into the bulk is much greater than the length of the cone, this problem can be treated as an infinite domain (axially) where the charge density goes to zero at long distances. The solution of eq 1 in an infinite domain is given by[20]

$$\rho(x,t) = \frac{q}{\sqrt{4\pi Dt}} e^{-x^2/4Dt} \tag{2}$$

The two relevant scales in this equation are the length scale λ and the time scale $1/f$, corresponding to the period of an ac cycle. For an acidified solution containing protein molecules, with a diffusion coefficient $D \sim 10^{-6}$ cm^2/s[21] and conductivity $\sim$100 μS/cm, the double layer thickness is $\lambda \sim 10^{-5}$ cm. The corresponding Maxwell relaxation time scale (or alternatively, the diffusion time scale) is given by λ^2/D and is approximately 10^{-4} s, an order of magnitude less than the time scale corresponding to the inverse of frequency ($f \sim$ 100 kHz). Thus, in the limit $1/f \ll \lambda^2/D$, the pre-exponential factor dominates the exponential term in eq 2. Therefore, for these ac fields the charge density, ρ, should scale as the inverse of the square root of the half period,

$$\rho \sim 1/\sqrt{t} \tag{3}$$

Since the frequency f is the reciprocal of this time scale t, $f \sim t^{-1}$, the charge distribution in the cone after each cathodic half cycle will scale as

$$\rho \sim f^{1/2} \tag{4}$$

Over the course of N ac periods (or half periods), the total accumulated ion concentration in the cone can be approximated by a summation

$$\rho_N = \sum_N \rho = N\rho \tag{5}$$

For a given time T, the number of periods is proportional to the ac frequency, $N \sim f$. Thus, the net ion accumulation over many periods will be the product of $\rho_N \sim ff^{1/2}$ or

$$\rho_N \sim f^{3/2} \tag{6}$$

From earlier visualization, droplets eject from the cone at a frequency of $\sim$100−1000 Hz, corresponding to approximately $\sim$100−1000 ac periods. These droplets will eject the accumulated charge ρ_N of the many ac periods, leading to a current i. The current, therefore, should follow a similar scaling behavior as the ion concentration such that

$$i \sim f^{3/2} \tag{7}$$

The inset of Figure 5 shows a measured current plotted as a function of $f^{3/2}$ along with linear curve fits, confirming this scaling theory and lending confidence to the mechanism that charges are created and entrained in the ac cone.

Frequency Effect on Ionization Suppression. One important potential application of this frequency-dependent entrainment in ac ESI could come in the form of reducing problems induced by ionization suppression widely observed in dc ESI

dx.doi.org/10.1021/ac103189p |*Anal. Chem.* 2011, 83, 3017–3023

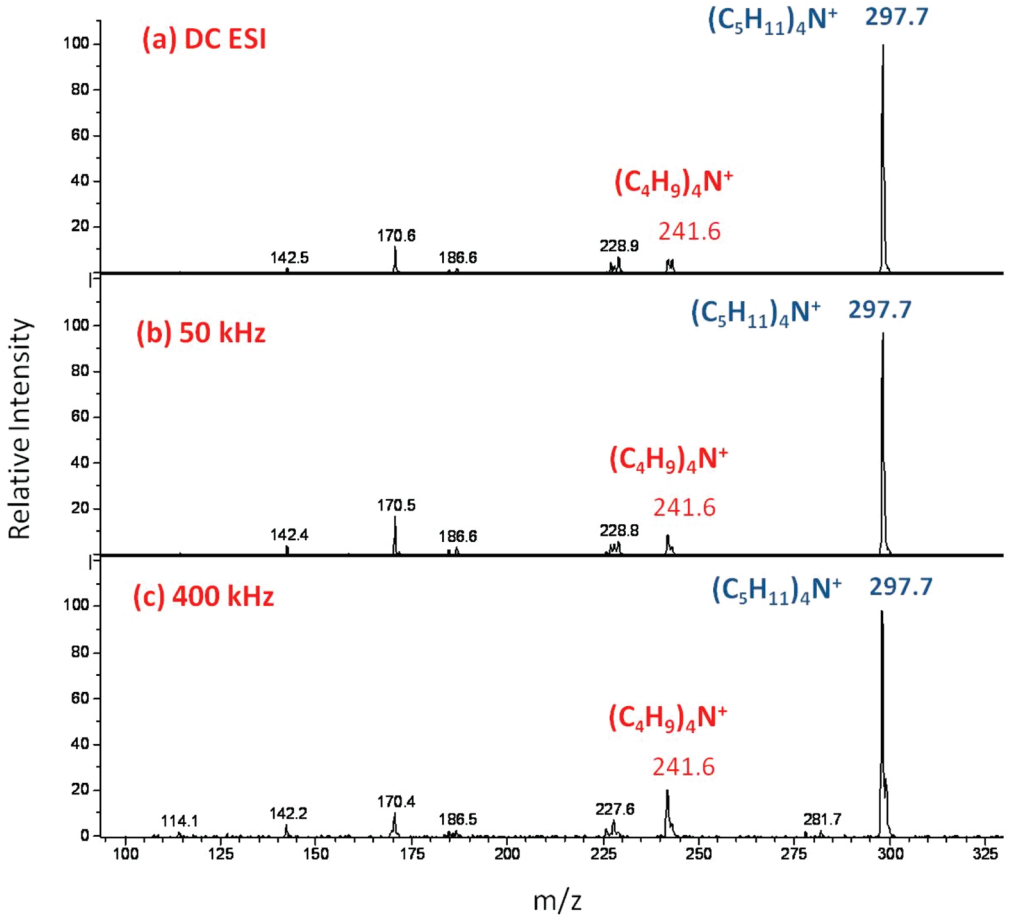

Figure 6. Mass spectra of equimolar mix of $(Butyl)_4N^+I^-$ (m/z = 241.7) and $(Pentyl)_4N^+I^-$ (m/z = 297.7) at (a) dc voltage of 2 kV, (b) 50 kHz and 1.1 kV_{rms}, and (c) 400 kHz and ~0.6 kV_{rms}.

mass spectrometry.[22,23] In dc ESI, the conventional understanding is that molecular ions are formed either through desorption from charged droplets (the ion evaporation model) or through Rayleigh fission. In either of these two mechanisms, if there are two (or more) analyte molecules in a droplet, there is competition between the molecules for ion formation, which leads to suppression of ion peaks in the mass spectrum. This is often attributed to differences in the surface activities and/or sizes of the two molecules. The finite number of charges in the droplet are often assumed to relax perfectly to the surface, and the more hydrophobic molecule screens the more hydrophilic molecule from access to the charges, limiting ionization.[24] On the other hand, current understanding of ac ESI is that the ionization reactions occur predominantly in the cone itself, as opposed to through droplet chemistry. One potential implication of this "cone ionization" mechanism is that it could mitigate the droplet chemistry that results in ionization suppression.

To study this effect, an equi-molar mixture of two surfactant molecules $(Butyl)_4N^+I^-$ (m/z = 241.7) and $(Pentyl)_4N^+I^-$ (m/z = 297.7) with different surface activities was studied. For small molecules, ion evaporation has been proposed as the dominant ionization mechanism in dc ESI. On the basis of this mechanism, the Thomson−Irabarne model[23] predicts that the ratio of the mass spectrum intensities for two analyte molecules should be the ratio of their gas phase ion sensitivity coefficients, which is directly proportional to the surface activity of the respective molecular ions. That is, the ratio of intensities I of the tetraalkylammonium ions should be

$$\frac{I[(Pentyl)_4N^+]}{I[(Butyl)_4N^+]} = \frac{k_p}{k_b} \quad (8)$$

where k_p and k_b are the gas phase ion sensitivity coefficients of the pentyl and butyl tetraalkylammoniums, respectively. If the molecule with higher surface activity, and thus a greater tendency to ionize, is in the numerator, eq 8 will give a ratio >1. If surface activity plays no role, then this ratio should tend toward 1 for an equimolar mixture, implying no ionization suppression. Since $(Pentyl)_4N^+I^-$ has a greater surface activity than $(Butyl)_4N^+I^-$, it should suppress the $(Butyl)_4N^+I^-$ signal, and this is clearly evident in the dc ESI mass sprectum shown in Figure 6a, in which the ratio of intensity of the two ions $(I[(Pentyl)_4N^+])/(I[(Butyl)_4N^+]) \sim 10$. Low frequency (<150 kHz) ac ESI behavior, as shown in Figure 6b closely resembles the dc ESI spectra. However, as evident from Figure 6c and Table 1, at much higher frequencies (>250 kHz), the ratio reduces to $(I[(Pentyl)_4N^+])/(I[(Butyl)_4N^+]) \sim 4$. This suggests that at high frequency, ac ESI reduces the role that surface activity plays during ionization. Since the ac field would play little role in ion evaporation ionization from the droplets, these results imply that the ionization is not occurring in the droplets emitted by ac electrospray and that "cone-ionization" mechanism is at play. Conceptually,

Table 1. Variation of the Ratio of MS Intensity of $(Pentyl)_4N^+I^-$ to $(Butyl)_4N^+I^-$ with ac Frequency

frequency (in kHz)	$(I(Pentyl_4N^+))/(I(Butyl_4N^+))$
80	11.2 ± 0.65
150	10.9 ± 0.96
200	10.97 ± 0.98
250	6.66 ± 0.12
300	5.31 ± 0.15
400	4.48 ± 0.11

this can be explained in the following manner. In droplet chemistry, ionization suppression is due to analyte molecules competing for a finite number of charges in the droplet. In the cone chemistry of an ac electrospray, however, the analyte molecules have access to more charges since they are replenished from the bulk solution every half cycle at a much faster rate (~100 kHz) than droplets are ejected (~100−1000 Hz). As such, surface activity plays a smaller role in ac ESI and ionization suppression is reduced. However, it should be noted that since the ratio did not decrease to a ratio of unity but only decreased by a factor of 2, there is likely still droplet chemistry occurring to create analyte ions in ac ESI but that the predominant ionization is likely occurring in the cone itself.

CONCLUSIONS

Higher order qualitative features of frequency dependent characteristics of ac ESI mass spectrometry are reported and are supplemented by voltage and current measurements and appropriate scaling laws. Three distinct voltage/frequency regimes of ac ESI behavior are identified, including the disappearance of analyte peaks at voltages higher than a threshold voltage. In addition, the charge state distribution in the resulting mass spectra can be distorted by the operating frequency, and at higher frequencies, a skewed Gaussian profile is obtained. By comparison to dc ESI at varying pH, the ac ESI effect is attributed to a local pH modulation in the cone itself that occurs due to the increased number of half cycles at higher frequencies. The effect of increased frequency is affirmed through current/voltage measurements that showed a distinct dependence on frequency as $f^{3/2}$, which is a result from the preferential entrainment of low mobility ions in the ac cone. Additionally, by ionizing predominantly in the cone itself, ac ESI reduces the detrimental effects of ion suppression frequently observed in dc ESI. This likely will form the pivotal role of ac ESI in MS applications in the future.

ASSOCIATED CONTENT

Supporting Information. This material is available free of charge via the Internet at http://pubs.acs.org.

AUTHOR INFORMATION

Corresponding Author

*D.B.G.: e-mail, dgo@nd.edu; phone, +1-574-631-8394; fax, +1-574-631-8341. H.-C.C.: e-mail, hchang@nd.edu; phone, +1-574-631-5697; fax, +1-574-631-8366.

ACKNOWLEDGMENT

N.C. and H.-C.C. wish to acknowledge financial support from Grant NSF-IDBR0852741 and the Center for Applied Mathematics at the University of Notre Dame, Notre Dame. D.B.G. would like to acknowledge funding from the University of Notre Dame Faculty Scholarship Award. N.C. would like to thank Dr. Matthew Champion and Dr. William Boggess (Department of Chemistry and Biochemistry, University of Notre Dame) for useful technical discussion and insight.

REFERENCES

(1) De la Mora, J. F. *Annu. Rev. Fluid Mech.* **2007**, *39*, 217–243.
(2) Marginean, I; Nemes, P.; Vertes, A. *Phys. Rev. Lett.* **2006**, *97* (1−4), 064502.
(3) Wilm, M. S.; Mann, M. *Int. J. Mass Spectrom. Ion Processes* **1994**, *134*, 167–180.
(4) Saville, D. A. *Annu. Rev. Fluid Mech.* **1997**, *29*, 27–64.
(5) Fenn, J. B.; Mann, M.; Meng, C. K.; Wong, S. F.; Whitehouse, C. M. *Science* **1989**, *246*, 64–71.
(6) Miranker, A.; Robinson, C. V.; Radford, S. E.; Dobson, C. M. *FASEB J.* **1996**, *10*, 93–101.
(7) Taylor, G. I. *Proc. R. Soc. London A* **1964**, *280*, 383–397.
(8) Ganan-Calvo, A. M. *Phys. Rev. Lett.* **1997**, *79*, 217–220.
(9) Lopez-Herrea, J. M.; Barrero, A.; Lopez, A.; Loscertales, I. G.; Marquez, M. *Aerosol Sci.* **2003**, *34*, 535–552.
(10) Ganan-Calvo, A. M.; Davilla, J.; Barrero, A. *J. Aerosol Sci.* **1997**, *28*, 249–275.
(11) Maheshwari, S.; Chang, H. -C. *Appl. Phys. Lett.* **2006**, *89* (1−3), 234103.
(12) Maheshwari, S.; Chang, H. -C. *J. Appl. Phys.* **2007**, *102* (1−6), 034902.
(13) Chetwani, N.; Maheshwari, S.; Chang, H.-C. *Phys. Rev. Lett.* **2008**, *101* (1−4), 204501.
(14) Chetwani, N.; Cassou, C. A.; Go, D. B.; Chang, H.-C. *J. Am. Soc. Mass Spectrom.* **2010**, *21*, 1852–1856.
(15) Basuray, S.; Chang, H.-C. *Phys. Rev. E* **2007**, *75*, 060501–060504.
(16) Christoni, S.; Bernardi, L. R.; Biunno, I.; Guidugli, F. *Rapid Commun. Mass Spectrom.* **2002**, *16*, 1686–1691.
(17) Supporting Information showing the dc ESI mass spectra for myoglobin obtained at ~2 kV and different pH.
(18) Feng, R.; Konishi, Y. *J. Am. Soc. Mass Spectrom.* **1993**, *4*, 638–645.
(19) Guevremont, R.; Siu, K. W. M.; Le Blanc, J. C. Y.; Berman, S. S. *J. Am. Soc. Mass Spectrom.* **1992**, *3*, 216–224.
(20) Evan, L. C. *Partial Differential Equations*; American Mathematical Society: Providence, RI, 1998.
(21) Wittenberg, B. J.; Moreno, V. R. *J. Biol. Chem.* **1972**, *247* 895–901.
(22) Tang, L.; Kebarle, P. *Anal. Chem.* **1993**, *65*, 3654–3668.
(23) Kebarle, P.; Tang, L. *Anal. Chem.* **1993**, *65*, 972–986.
(24) Zhou, S.; Cook, K. D. *J. Am. Soc. Mass Spectrom.* **2001**, *12* 206–214.